NASA Technical Memorandum 83237

USE OF A VARIABLE EXPOSURE PHOTOGRAPHIC PYROMETER TO MEASURE SURFACE TEMPERATURES ON A HEMISPHERICAL-FACE MODEL

ANDRONICOS G. KANTSIOS, WILLIAM C. HENLEY, JR.
AND WALTER L. SNOW

April 1982

NASA

National Aeronautics and
Space Administration

Langley Research Center
Hampton, Virginia 23665

USE OF A VARIABLE EXPOSURE PHOTOGRAPHIC PYROMETER
TO MEASURE SURFACE TEMPERATURES ON A
HEMISPHERICAL-FACE MODEL

Andronicos G. Kantsios, William C. Henley, Jr. and
Walter L. Snow

SUMMARY

Remote surface temperature measurement devices have come into common usage in the past few years. The use of infrared devices in satellite measurements, ground wind tunnel facilities, and industry have clearly proved advantageous. One early instrument in this measurement area (especially in wind tunnel/arc tunnel work) has been the photographic pyrometer. When used for the visible portion of the spectrum the technique is limited to the high temperature range where objects become self luminous. For such cases, the advantage of visible records outweigh many of the disadvantages of working with film. The paper will discuss the use of such an instrument in a wind tunnel test pointing out its advantages and disadvantages and will discuss recent innovations which promise to make the readup more tractable.

INTRODUCTION

The testing of aerodynamic vehicle configurations requires the use of many measurement systems to define such parameters as pressure, temperature, and gas flow. One parameter of great importance in material studies is the surface temperature. Thermocouples are generally used but often the optimum location of these sensors cannot be predetermined nor can all desired locations be sampled. The radiometer, especially the wide field radiometer (in this case a photographic pyrometer), can scan the entire area of interest without disturbing the test article.

A spherical dome design (figure 1) which is going to be used on the space shuttle vertical stabilizer as a housing for an infrared camera system was tested at the 8-foot High Temperature Structures Tunnel of Langley Research Center to verify the three-dimensional analytical model for predicting surface temperature on the dome. The test dome is full scale with two window ports through which the infrared camera will observe the lee-side of the shuttle during entry. The dome is covered with insulating tiles similar in shape, size, and material to that used on the space shuttle. The window frames were carbon phenolic ablators and the windows are simulated with metal which has been coated to increase the emittance.

Two tests were conducted. The first was a radiative test using quartz lamp heaters to raise the surface temperatures while the second used aerodynamic heating with the tunnel in operation. Temperatures were monitored during the simulations by both thermocouples placed at preselected points on the surfaces

and interior of the model, and by a scanning infrared radiometer to observe the entire model, while a photographic pyrometer with close-up lens observed the temperature profile at the stagnation window area.

The photographic pyrometer and the data derived from it will be discussed in this paper and comparison with thermocouple data will be made as appropriate.

SYMBOLS

A   area, m^2

D   photographic density $\equiv -\text{Log}_{10} \tau$

E   spectral irradiance, $W/(m^2\text{-nm})$

L   spectral radiance, $W/(m^2\text{-sr-nm})$

Q   radiant energy, J

R   film responsivity, Signal/J

S   "signal" from a detector, e.g., photographic density D

T   absolute temperature, K

t   time, s

x   coordinate, m

y   coordinate, m

ε emittance of surface

θ polar angle

λ wavelength, nm

τ transmission

τ^* propagance

ϕ azimuthal angle

Ω projected solid angle, sr

ω solid angle, sr

i   ith frame in camera and filter wheel location

Q   radiant input

t   true

λ spectral

Superscripts

m   model

o   blackbody

s   standard

Theory

Photographic pyrometry attempts to correlate the transmission of a
negative film image with the temperature dependent radiance of the object which
produced it. It is convenient to compress the scale and deal with the common
logarithm of transmission or more precisely

$$D \equiv -Log_{10} \tau \qquad\qquad (1)$$

where τ is the transmission and D is called, for historical reasons, the
(photographic) density. Modifying adjectives for this quantity relate to the
manner in which the transmission is measured. In this paper, specular density
is used.

A minimum threshold or irradiance is required to expose the film.
Irradiance levels exceeding this threshold value by (usually) several orders of
magnitude are said to "saturate" the film since all of the potential chemical
photoreceptors are exhausted and become insensitive to further photon activa-
tion. The relevant independent variable in photography is the exposure which
is a measure of the photon flux into a given area of the film multiplied by
the exposure time. A typical curve of specular density versus log exposure
is shown in figure 2. The mathematical domain of abscissa values is commonly
referred to as the film latitude and will depend to some extent on processing.
To accommodate higher exposure levels the scene can be viewed through neutral
density filters, the effect being to translate the D vs. log exposure or
characteristic curve along the exposure axis.

The custom-made pyrometer used for this test is described in referenece 1 and
is shown in figure 3. This specialized camera is equipped with a shutter-
synchronized rotating neutral density filter whose transmittance varies from

nearly 100 percent to 0.003 percent in 18 steps. This range virtually insures that several exposures of an 18 frame sequence will be in the usable portion of the film characteristic. Another feature of the photographic pyrometer which distinguishes it from its disappearing filament counterpart is the wavelength bandpass. The disappearing filament pyrometer incorporates a relatively narrow band filter centered at 650 nm. The spectral selectivity of the photographic pyrometer is determined by the film response which is broad band; this more efficient use of radiant energy encumbers the interpretation slightly by requiring the use of an auxiliary "master" curve (see reference 1).

The "master" curve is the key to quantitative interpretation of the data so its derivation will be given. Film responds to radiant energy and its responsivity (R_Q) may be written as

$$R_Q = dS/dQ \quad [S \cdot J^{-1}] \tag{2}$$

where S is some "signal" such as transmission of the developed negative or more frequently the photographic density defined previously. The otherwise troublesome fact that the responsivity is affected by environmental and complex chemical processes is rendered tractable by using substitution standards for calibration.

Let $dE_\lambda (x, y, \theta, \phi) \; [W-m^{-2}-nm^{-1}]$ be the differential spectral irradiance on the film area element dA from a beam of spectral radiance $L_\lambda (x, y, \theta, \phi, \lambda) \; [W-m^{-2}-sr^{-1}-nm^{-1}]$ where x and y specify generic coordinates and θ, ϕ, the beam direction. Functionally

$$dE_\lambda = L_\lambda (x, y, \theta, \phi, \lambda) \cos \theta \, d\omega \quad [W-m^{-2}-nm^{-1}] \; dA \; [m^2] \tag{3}$$

with solid angle and wavelength, respectively, ω and λ. The exposure sequence consists of measuring the irradiance over a shutter time interval $\Delta t \, [s]$ and the film responsivity will convert this exposure to a "signal," S, which we will take to be synonymous with specular optical density. Mathematically,

$$dS = R_Q(\lambda) \; [S-J^{-1}] \; L_\lambda(x, y, \theta, \phi, \lambda) \; [J-s^{-1} \cdot m^{-2} - sr^{-1} - nm^{-1}]$$

$$\cos \theta \, d\omega \; [sr] \; \Delta t \; [s] \; d\lambda \; [nm] \; dA \; [m^2] \tag{4}$$

The radiance at the film plane is related to the radiance of the test surface by

$$L_\lambda (x, y, \theta, \phi, \lambda) = L_\lambda^m (x, y, \theta, \phi, \lambda) \cdot \tau_i^* \tag{5}$$

4

where the superscript m refers to "model" and τ^* is the propagance (reference 2) which involves attenuation in the optical path from source to film plane. In this experiment, τ^* is determined mainly by the neutral density wedge filter corresponding to frame i and its dependence in the response range of the film is essentially constant by virture of the design of the pyrometer and its filters. Therefore, no variable dependence is shown.

The net signal in the i-th frame is obtained by integrating over the solid angle (determined by camera aperture stops) and the wavelength such that

$$S^m = \tau^*_i \, \Delta t dA \int_\theta \int_\phi \cos \theta \, d\omega \int R_Q(\lambda) \, L^m_\lambda \, d\lambda \qquad (6)$$

In pyrometry measurements, the radiance of an object can be expressed in terms of blackbody radiance L^o_λ (assuming negligible reflection of energy from external sources) through a proportionally constant called the spectral emittance, $\varepsilon(\lambda)$ as

$$L_\lambda = \varepsilon(\lambda) \, L^o_\lambda \, (T, \lambda) \qquad (7)$$

The emittance then becomes the ratio of the radiance emitted by a surface to that emitted by a blackbody at the same surface temperature and wavelength.

Using the emittance relationship, the photographic pyrometer working equation then becomes

$$S^m = \tau^*_i \, \Delta t dA \, \Omega \int_\lambda R_Q(\lambda) \, \varepsilon^m(\lambda) \, L^o_\lambda \, (T, \lambda) \, d\lambda \qquad (8)$$

where $\Omega = \int_\theta \int_\phi \cos \theta d\omega$ is called the "projected" solid angle. For calibration, a standard source is substituted for the test surface and operated at true temperature T^S_t. Using the same frame

$$\frac{S^S(T^S_t)}{S^m(T^m_t)} = \frac{\int_\lambda R_Q(\lambda) \, \varepsilon^S(\lambda) \, L^o_\lambda \, (T^S_t, \lambda) \, d\lambda}{\int_\lambda R_Q(\lambda) \, \varepsilon^m(\lambda) \, L^o_\lambda \, (T^m_t, \lambda) \, d\lambda} \qquad (9)$$

This equation relates the measured film densities on the left hand side with a calculable function on the right. This relationship has been called a "master" curve in reference 1.

Calibration

The relationship between the optical density of the film and its exposure is determined by varying the exposure and observing the change in film density. A tungsten filament with an emittance of 0.45 (reference 3) is used as the source. Kodak Plus-X negative film whose relative spectral sensitivity between 400-700 nm as shown in reference 4 is used to record the test. Several calibration sequences were recorded on the test film. This film has the same relative spectral response as Tri-X pan over the same spectral interval (see reference 5). Tri-X pan data has been used to establish the film responsivity. An optical disappearing filament pyrometer was used to determine the tungsten filament temperature. The "master" curve corresponding to this test is shown in figure 4.

A film exposure calibration is determined by producing an 18 frame sequence of any test scene recorded by the photographic pyrometer with the filter varying the exposure over the 18 frames. Figure 2 shows the measured response to a sequence of the standard tungsten filament lamp. The arrow on the abscissa locates the exposure of the standard lamp through a specific filter at a specific frame number (frame two) which was used for the data reduction. The measurement of density at any point in the film negative allows the temperature to be estimated using figures 2 and 4.

Data and Its Interpretation

The sidewall of the center core in figure 1 was monitored by the photographic pyrometer. Thermocouples (whose location are shown in figure 5) also monitored the temperature of the conical walls. Figure 6 is a plot of the temperature time history of some of these thermocouples. At 47 seconds into the run, the model entered the flow stream and the thermocouples indicated the rise in temperatures. At 55 seconds, the T-24 and T-29 thermocouple failed as indicated by erratic behavior; at 64 seconds, T-25 also failed, while T-23 and T-26 thermocouples continued indicating throughout the period. The maximum temperatures indicated on the thermocouples prior to failure were in the 1140 - 1250K range. Without any additional information, the thermal performance of this model could not be monitored at these times for lack of sensors. Television and motion picture monitors, of course, may show superficial changes as could the photographic pyrometer. Figures 7, 8, 9, 10, and 11, visuallly indicate the sequence of events leading up to and following the thermocouple failures. The bright areas are those of higher temperature while the darker regions are cooler. In figure 7 (47.6 sec), indications of coating spall are evident as is the high temperature in the gap areas between insulation tile. Figure 8 (50.6 sec) shows a continued increase in temperature. In figure 9 (53.6 sec), a gap not even evident in figure 7 has become very luminous. On the surface, separation between tiles is becoming evident. This separated tile

6

contains thermocouple 24. Thermocouple 23 is in the spall area on the adjoining tile. In figure 10 (55.6 sec), the entire gap width has become heated and is at a higher temperature than the insulation. By the time of figure 11 (56.6 sec), the tile at the left side of the cone is gone. These five figures demonstrate the advantage of a camera with a variable density filter capability; data can be collected photographically over a broad range of exposure values without saturating the film.

Furthermore, as a pyrometer, temperature data can be collected by measuring the density of the photogrpahic film. A facsimile photograph indicating temperature variation in a field as a function of a particular code can be generated which not only provides temperatures, but also at a glance provides an overview of the thermal map of the scene. Figure 12 demonstrates how such a pattern may be set up. A scan line is taken across a portion of the model image and a raster-density encoder attached to the densitometer converts it to code. A conventional density sweep may result in a trace similar to the solid curve, but using the encoding scheme, a selectable density change ΔD is chosen so that the pen records either blanks, dots, or lines within the increment. The sequence dot-line-blank-dot . . . signified increasing density and reverses when the density decreases. The choice of density increment is somewhat arbitrary and is a compromise between too small where the code is indistinguishable due to rapid change, to the opposite extreme where insufficient resolution is available to make the image recognizable. A choice of 0.119D is shown in figure 2 and the legend corresponding to the coded isodensity trace is listed in the table.

TABLE

TEMPERATURE DECODING BASED ON EMITTANCE OF 0.8

T (K)	Code
1278-1300	blue-blank
1300-1317	blue-dot
1317-1331	blue-line
1331-1344	green-blank
1344-1361	green-dot
1361-1380	green-line
1380-1401	red-blank
1401-1422	red-dot
1422-1446	red-line
1466-1470	yellow-blank
1470-1500	yellow-dot
1500-1521	yellow-line

Color can then be added to this system to heighten the contrast and to improve visibility. A Joyce-Loebl Isodensitracer^R was used to acquire this data (figure 13). At a glance, the predominant temperatures of this model at this time vary from 1278 K to 1380 K with temperatures up to 1446 K at the gaps and in one area up to 1532 K. On closer examination, the dots and dashes will further break down the temperature to finer detail. Of course, if the specific

temperature at a specific point is desired, a density measurement of that point through the frame sequence will produce a temperature history similar to that of point sensors.

Thermocouple data consistently indicated lower surface temperatures than photographic pyrometry data. "Surface" thermocouples in ceramic materials are mounted in grooves and over coated with ceramic material which fills the groove. Figure 1 shows a smooth surface with no obvious thermocouples. The material above the thermocouple acts as an insulator causing the lower reading. On the other hand, surface emittance affects the radiance from the surface. If as seen in figure 9, spalling of the coating occurs, the surface temperature will drop initially, but will then increase to a value higher than the surroundings because the surface emittance is lower reducing the radiation heat loss. At this point without further extensive analysis, the discrepancy between the two temperature measuring approaches cannot be defined.

CONCLUDING REMARKS

Photographic pyrometry has been used as a non-intrusive method of measuring high temperatures. As with all pyrometers, effects of surface emittance, optical distortion, and atmosphere will have to be considered for quantitative comparison with other methods. Models whose unique surfaces make them difficult to instrument with thermocouples are often amenable to photographic methods.

Data reduction presently is difficult because of the hand labor required. However, computer operated densitometers or optical processors will eliminate the tedious nature of the data reduction and create a more acceptable instrument technique. An early semi-mechanical servo densitometer which generated the image as in figure 13 is a crude example of a potential automatically generated image.

Operating as it does in the visible spectrum with wide field of view makes this system easy to set up and use since it is basically a movie camera. In contrast, infrared scanning radiometers are more awkward to align and interpret. When coupled with modern image processing equipment, the optical pyrometer will resurface as a viable weapon in the arsenal of the measurement engineer.

8

REFERENCES

1. Exton, R. J.: "A Variable Exposure Photographic Pyrometer," ISA
   Transactions, Vol. 4, October 1965, pp. 364-373.

2. Nicodemus, Fred E., Editor: "Self-Study Manual on Optical Radiation
   Measurements," NBS Technical Note 910, 1978. Available from U.S.
   Government Printing Office, Washington, DC 20402.

3. Kaspar, J.: "Radiometry" in American Institute of Physics Handbook
   Edited by D. E. Gray, Third Edition, p. 6-212, McGraw-Hill, NY, 1972.

4. Eastman Plus-X Negative Film 5231 and 7231. Kodak Publication No.
   H-I-5231, Revised 1977.

5. Kodak Plates and Films for Scientific Photography. Kodak Publication P-315,
   p. 19d, 1973.
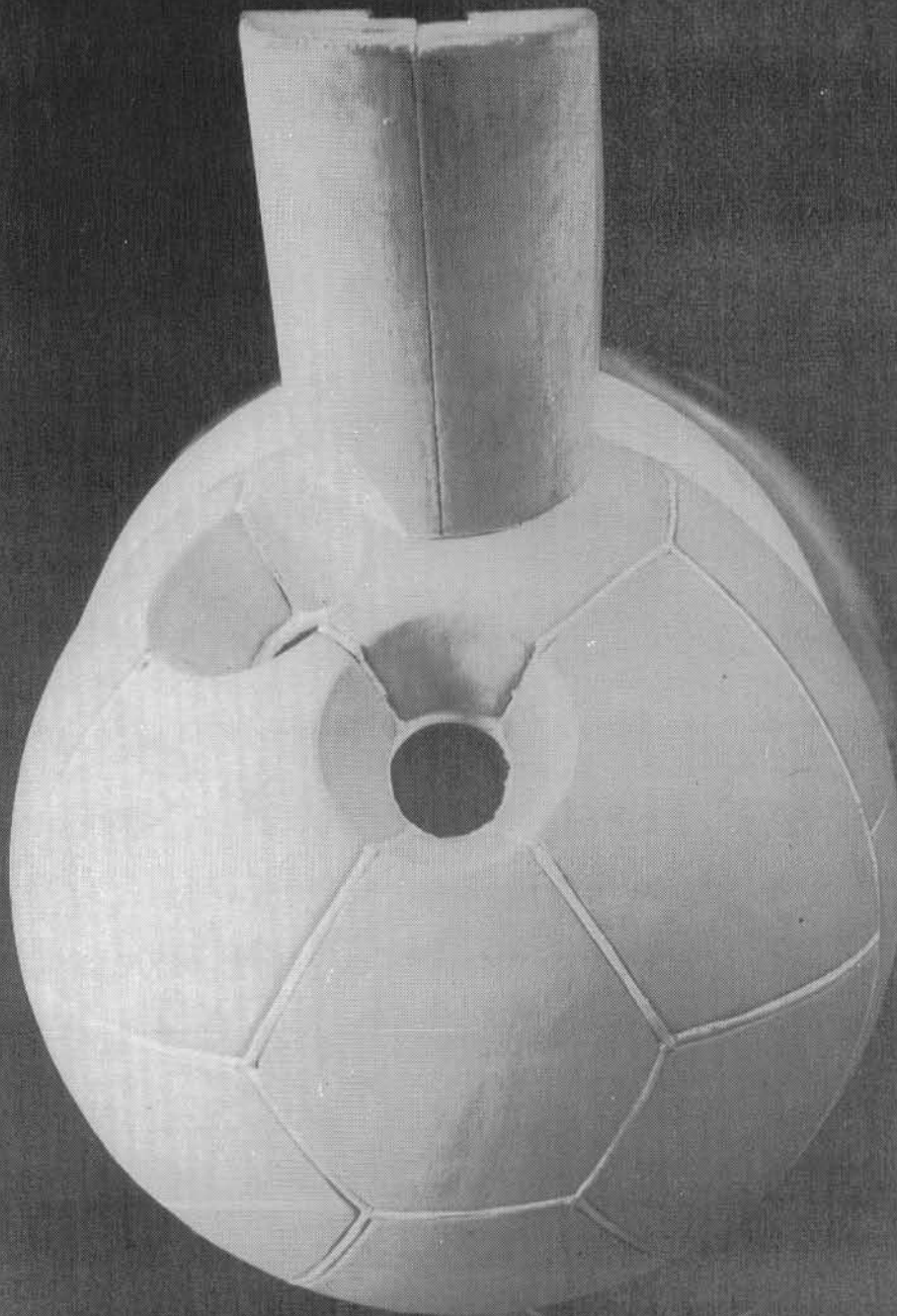
Figure 1.- Shuttle infrared camera housing.
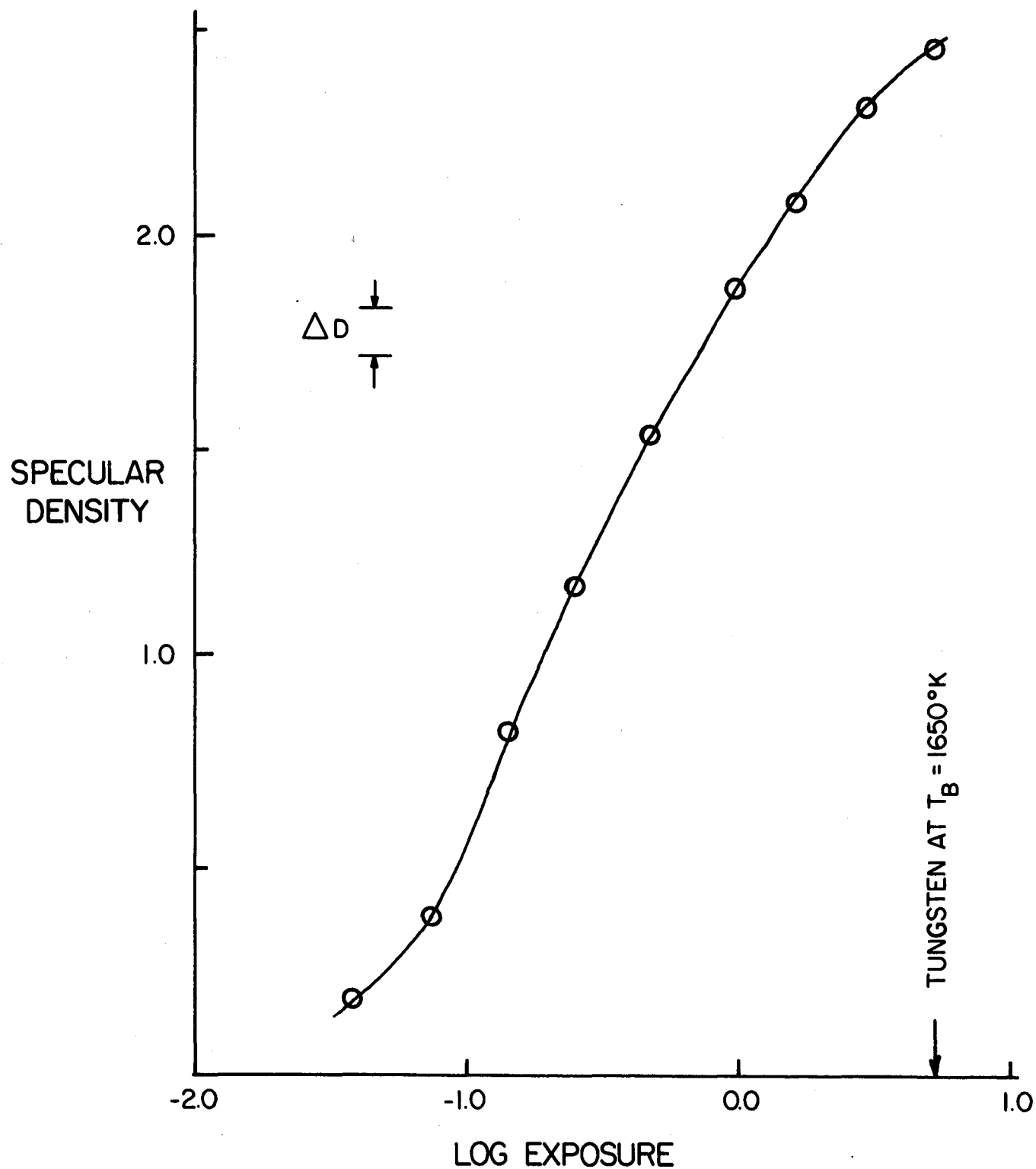
Figure 2.- Density-Log exposure curve for Plus-X negative film 5231. The
arrow indicates exposure of the tungsten filament operated at
brightness temperature 1370 K substituted for the model. The
isodensitracer increment is labeled as ΔD.

11
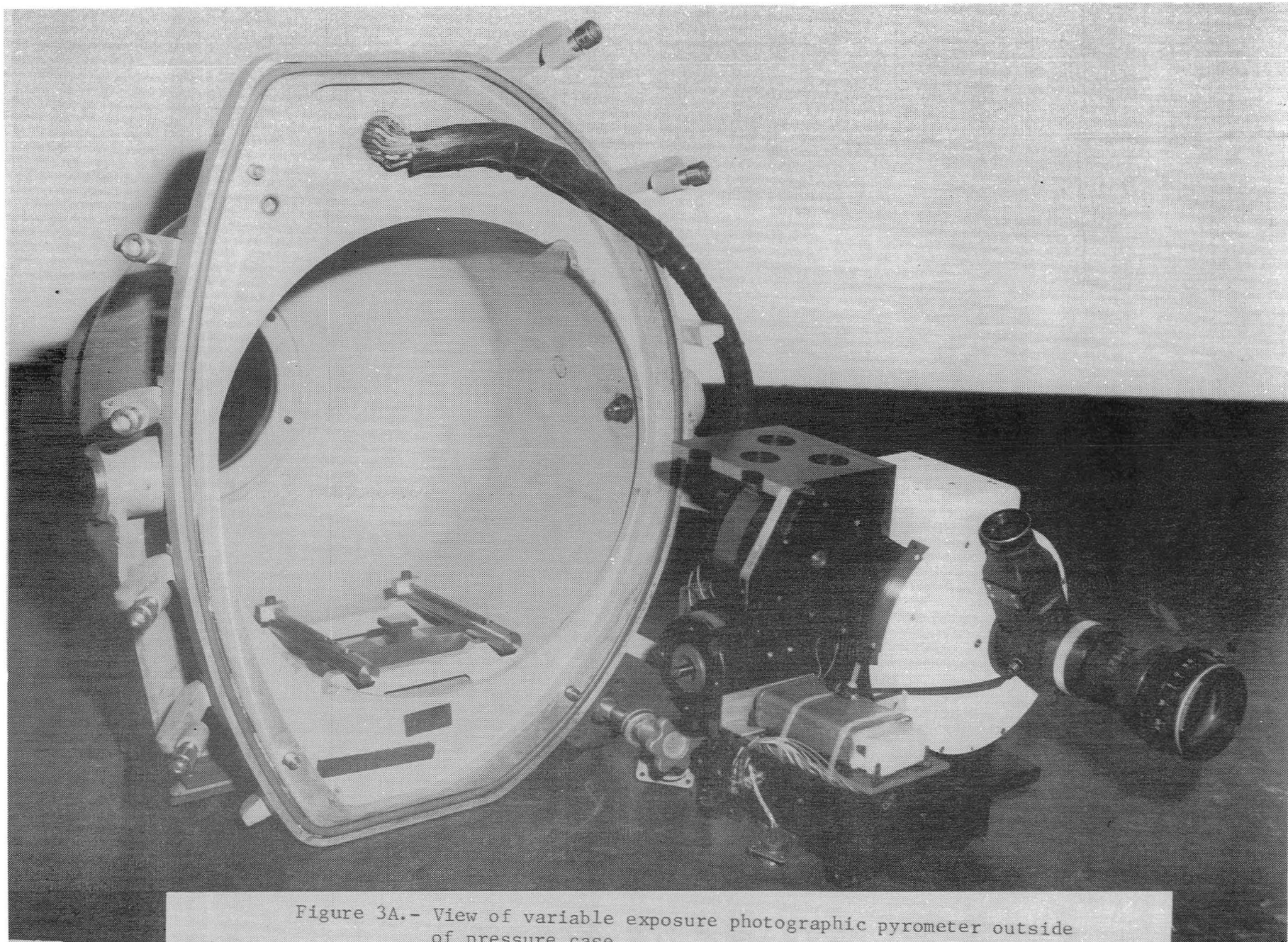
Figure 3A.- View of variable exposure photographic pyrometer outside of pressure case.
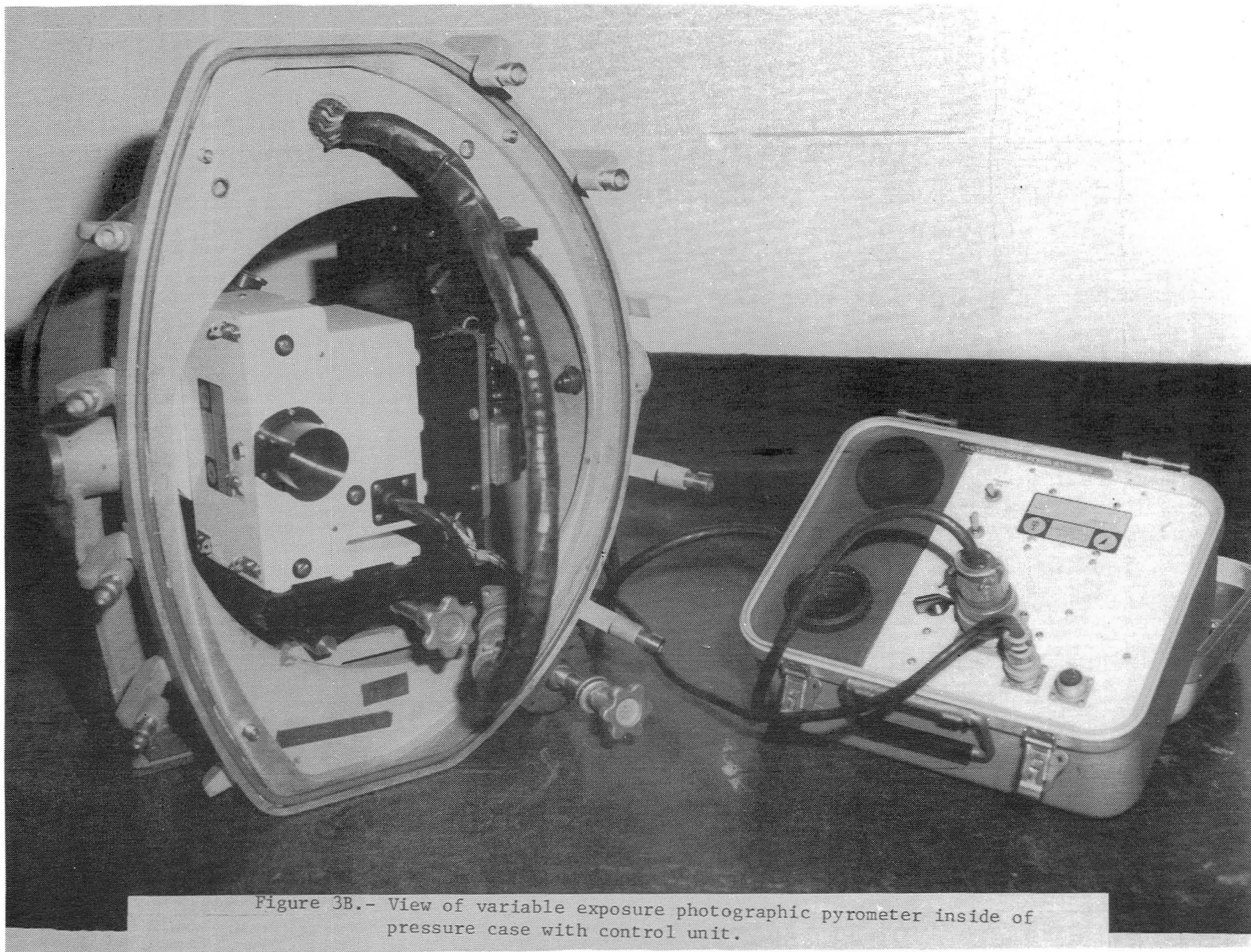
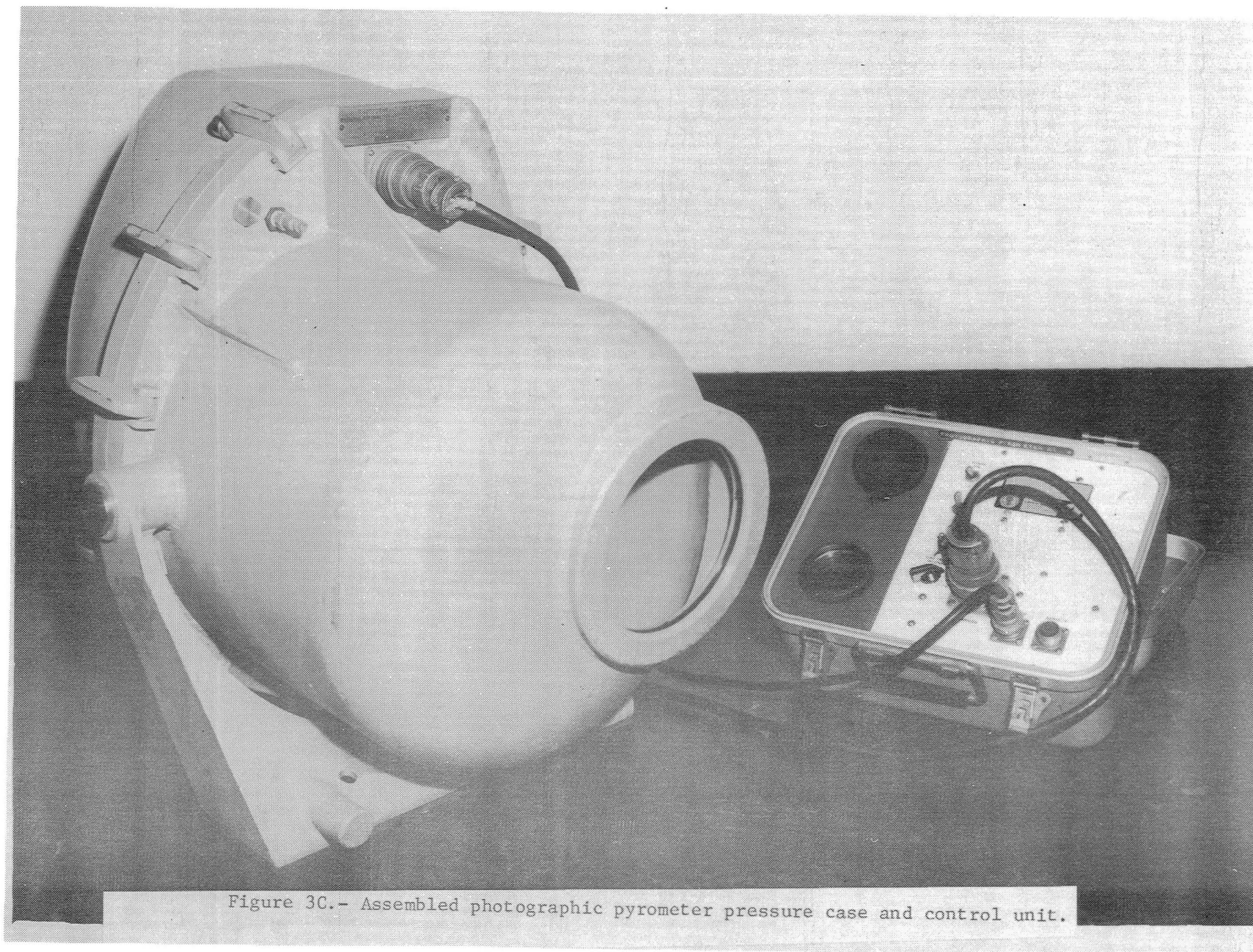Figure 3B.- View of variable exposure photographic pyrometer inside of pressure case with control unit.

Figure 3C.- Assembled photographic pyrometer pressure case and control unit.
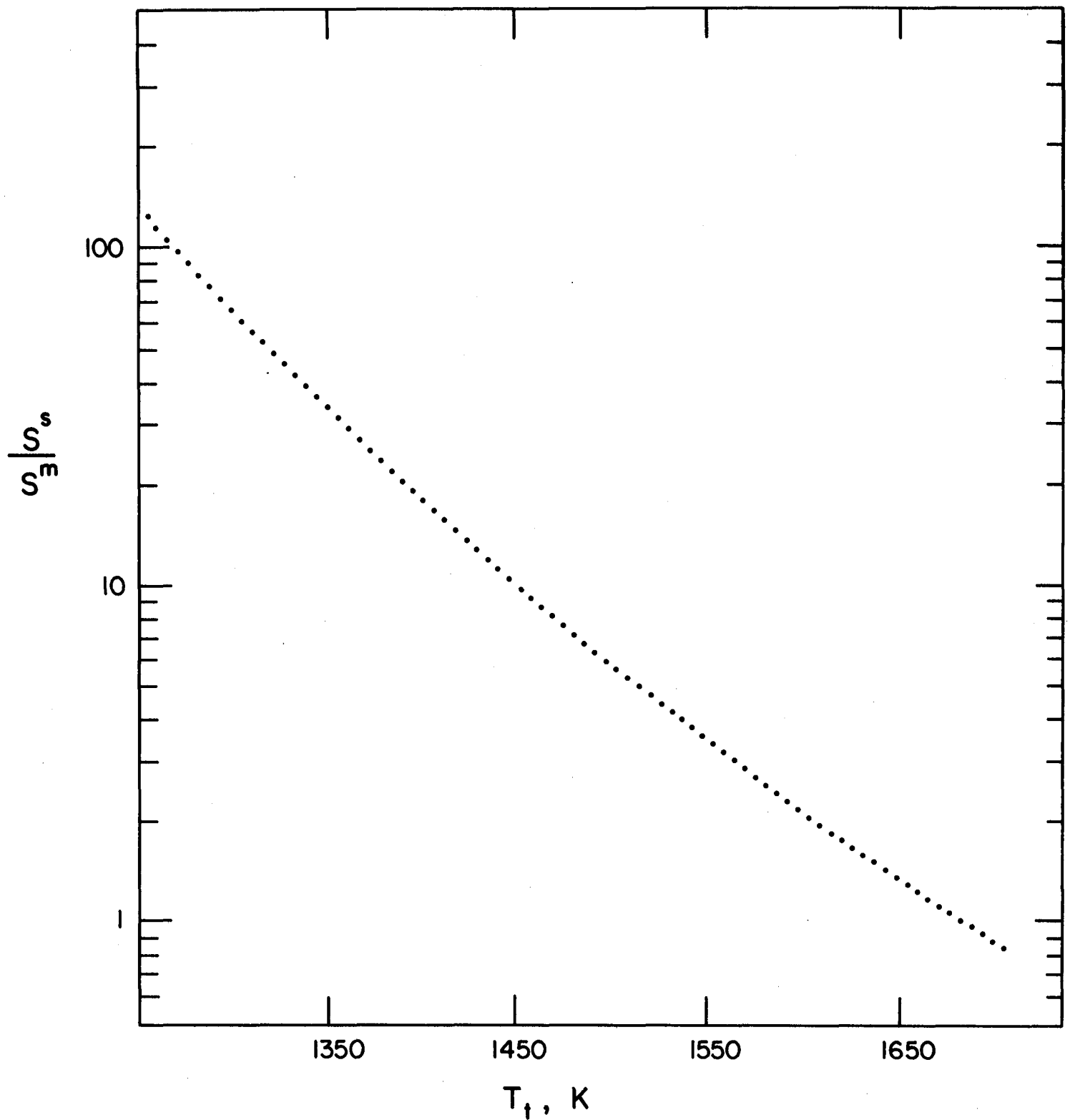
Figure 4.- "Master" curve based on assumed spectral emittance of 0.8 for test
surface m and tungsten standard at brightness temperature of 1644 K
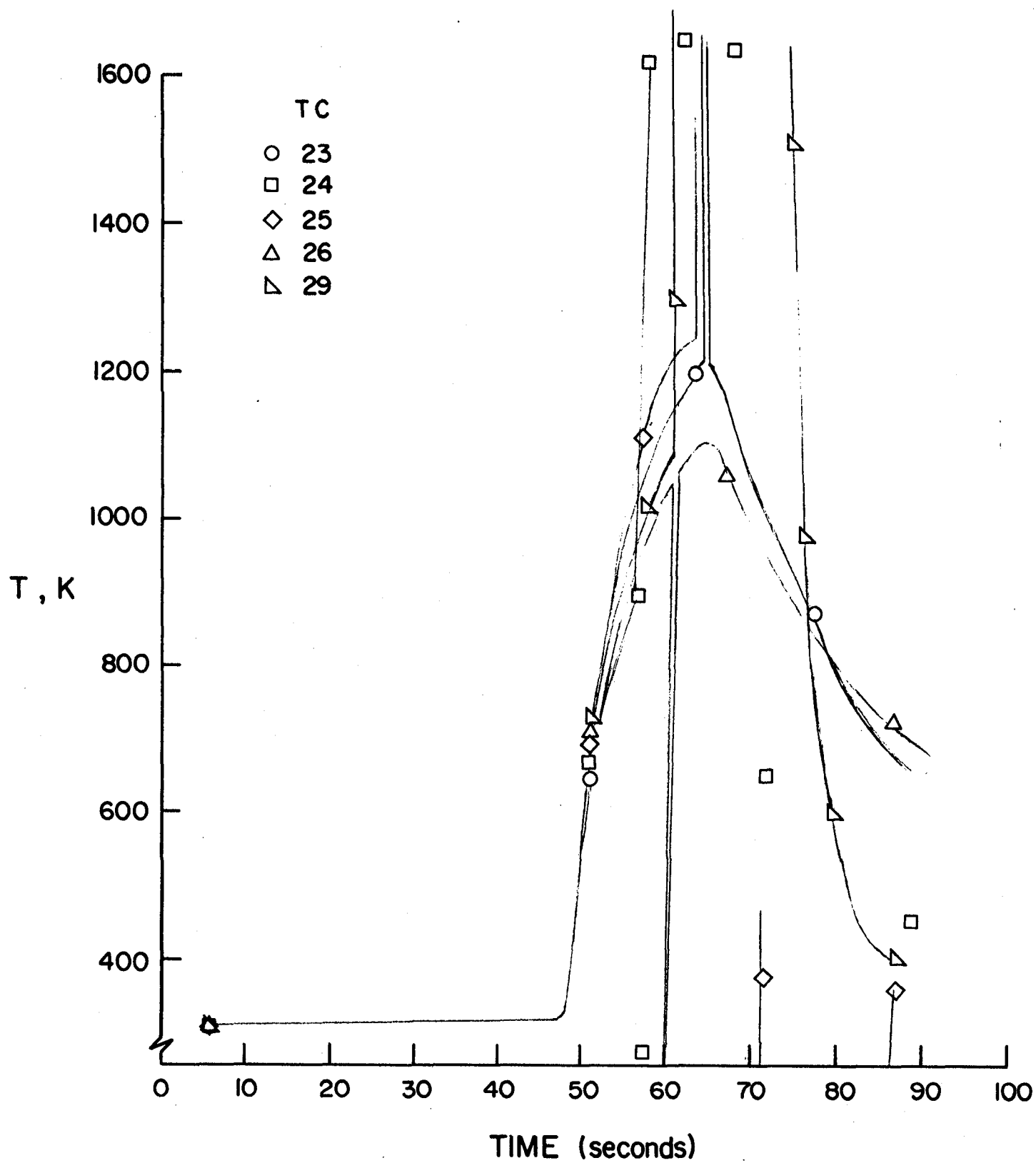corresponding to T_t = 1748 K.
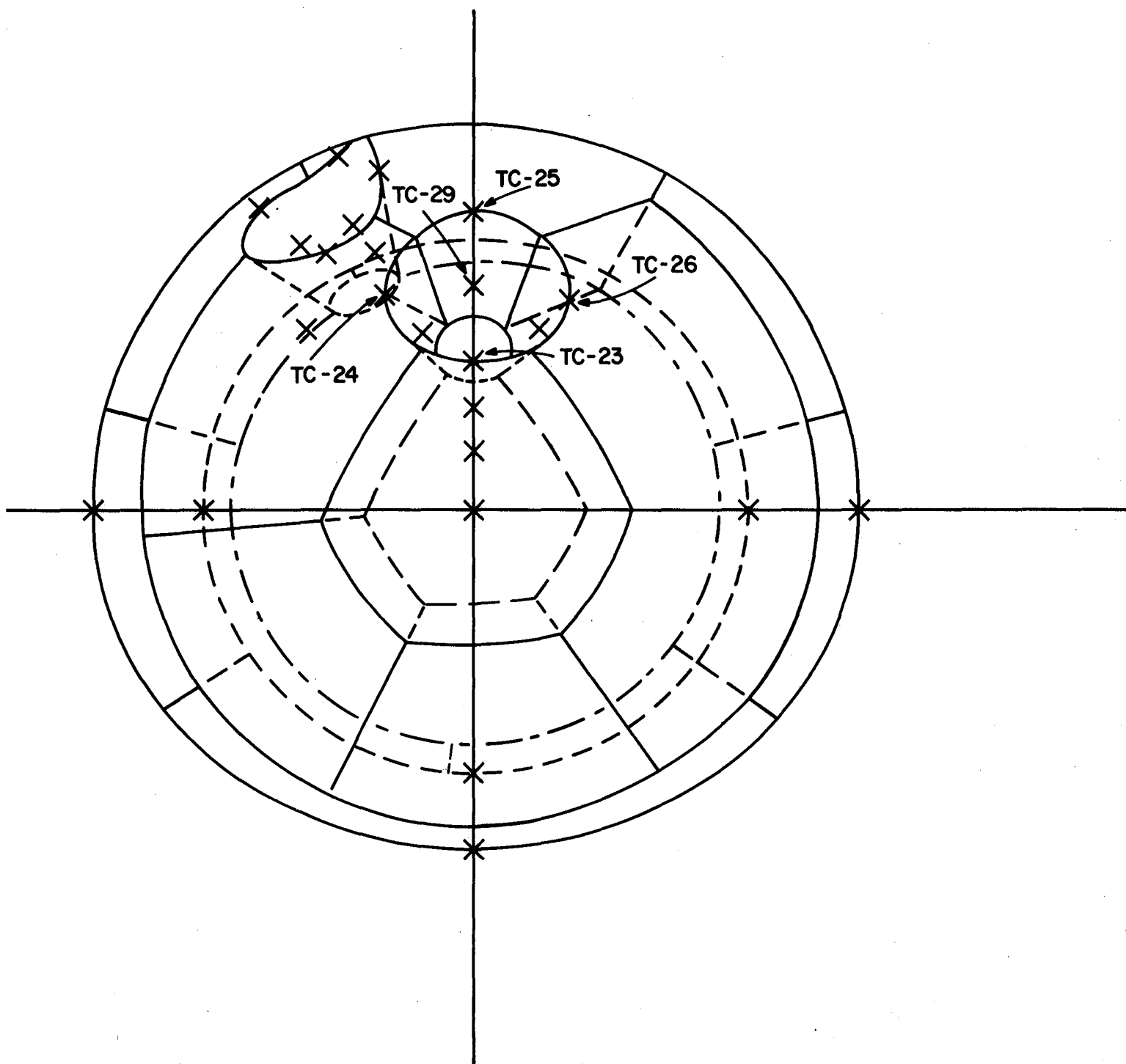
Figure 5.- Map of thermocouple locations.
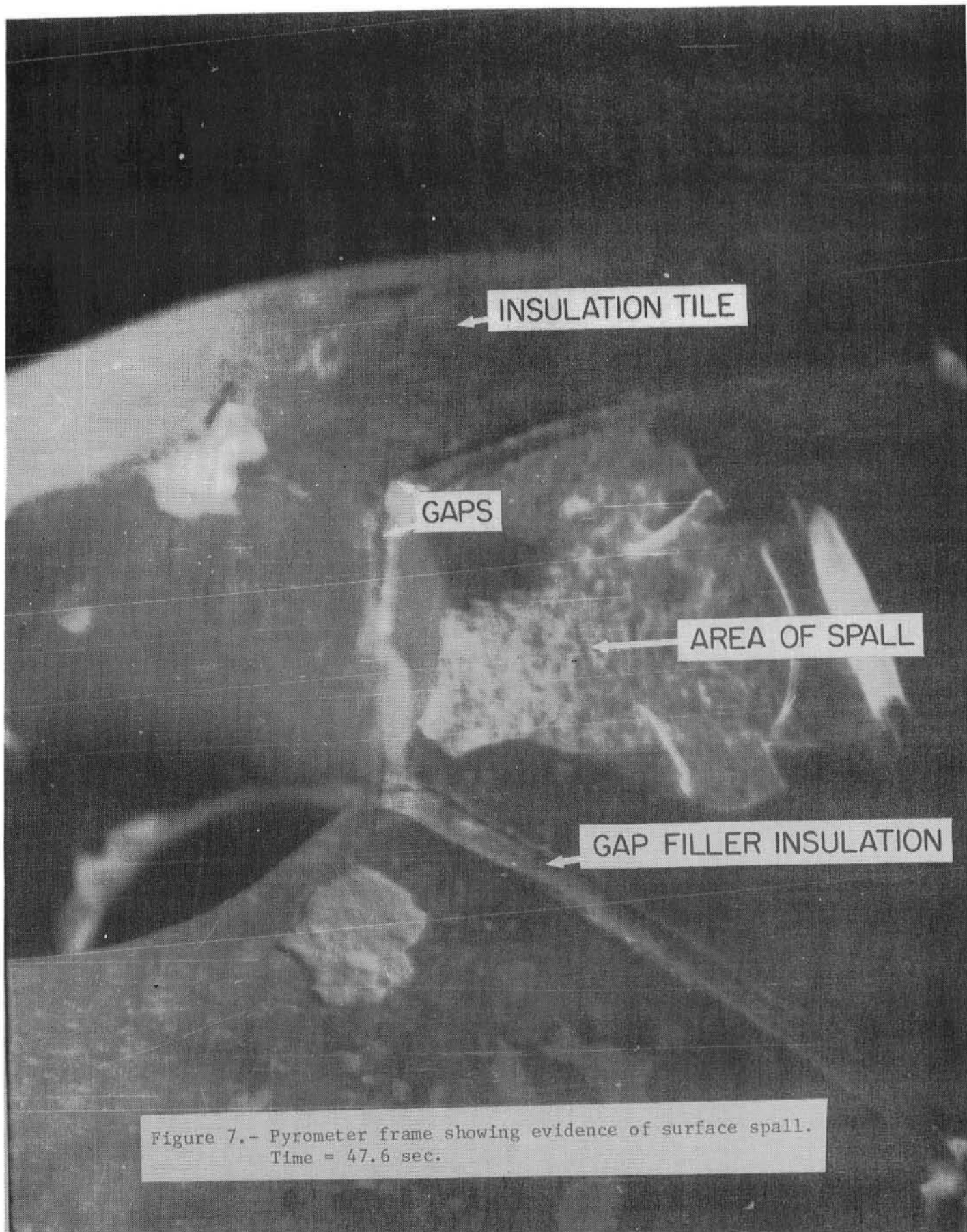
Figure 6.- Temperature history of thermocouples.

INSULATION TILE

GAPS

AREA OF SPALL

GAP FILLER INSULATION

Figure 7.- Pyrometer frame showing evidence of surface spall.
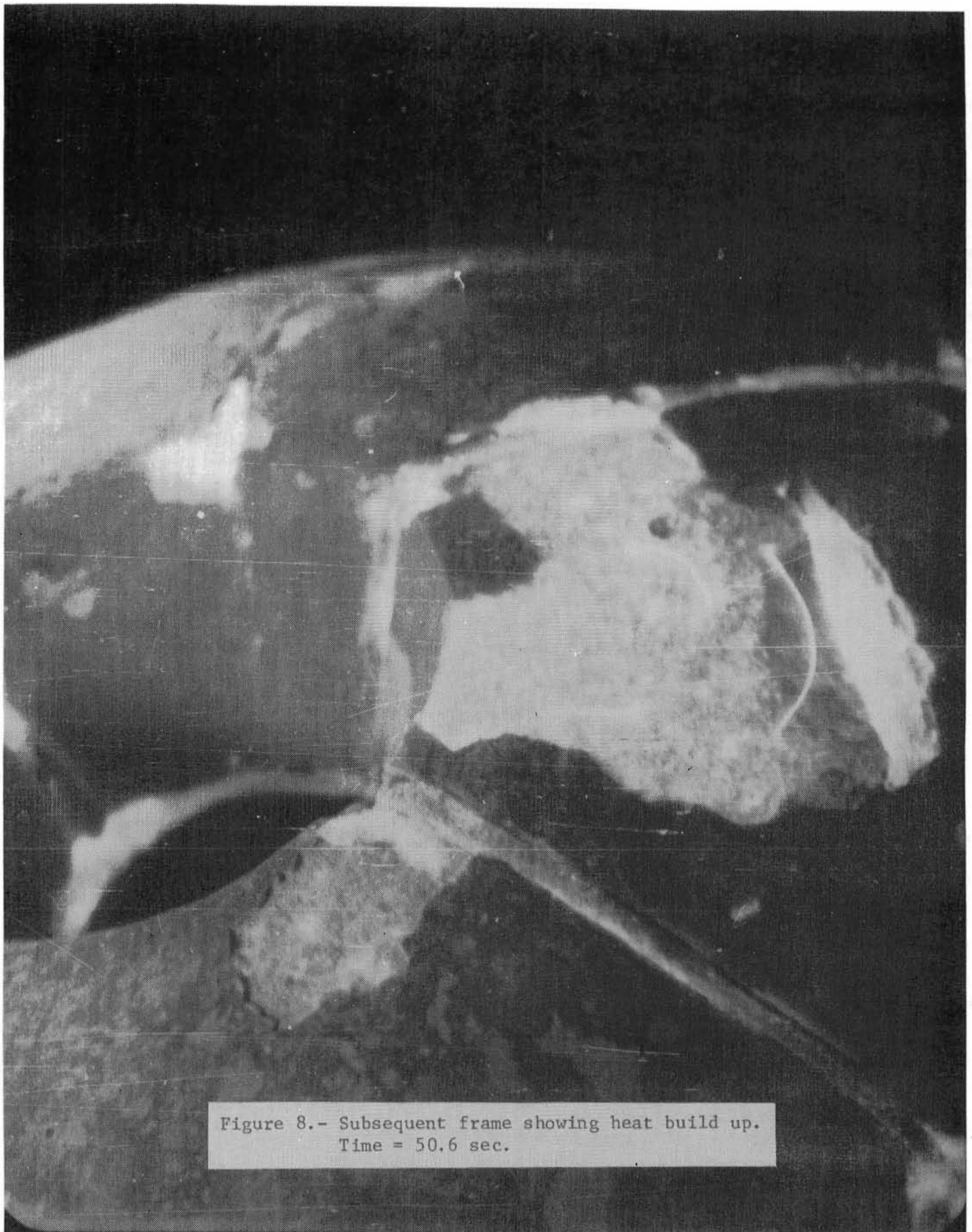Time = 47.6 sec.

Figure 8.- Subsequent frame showing heat build up.
Time = 50.6 sec.

NEW GAP FORMED

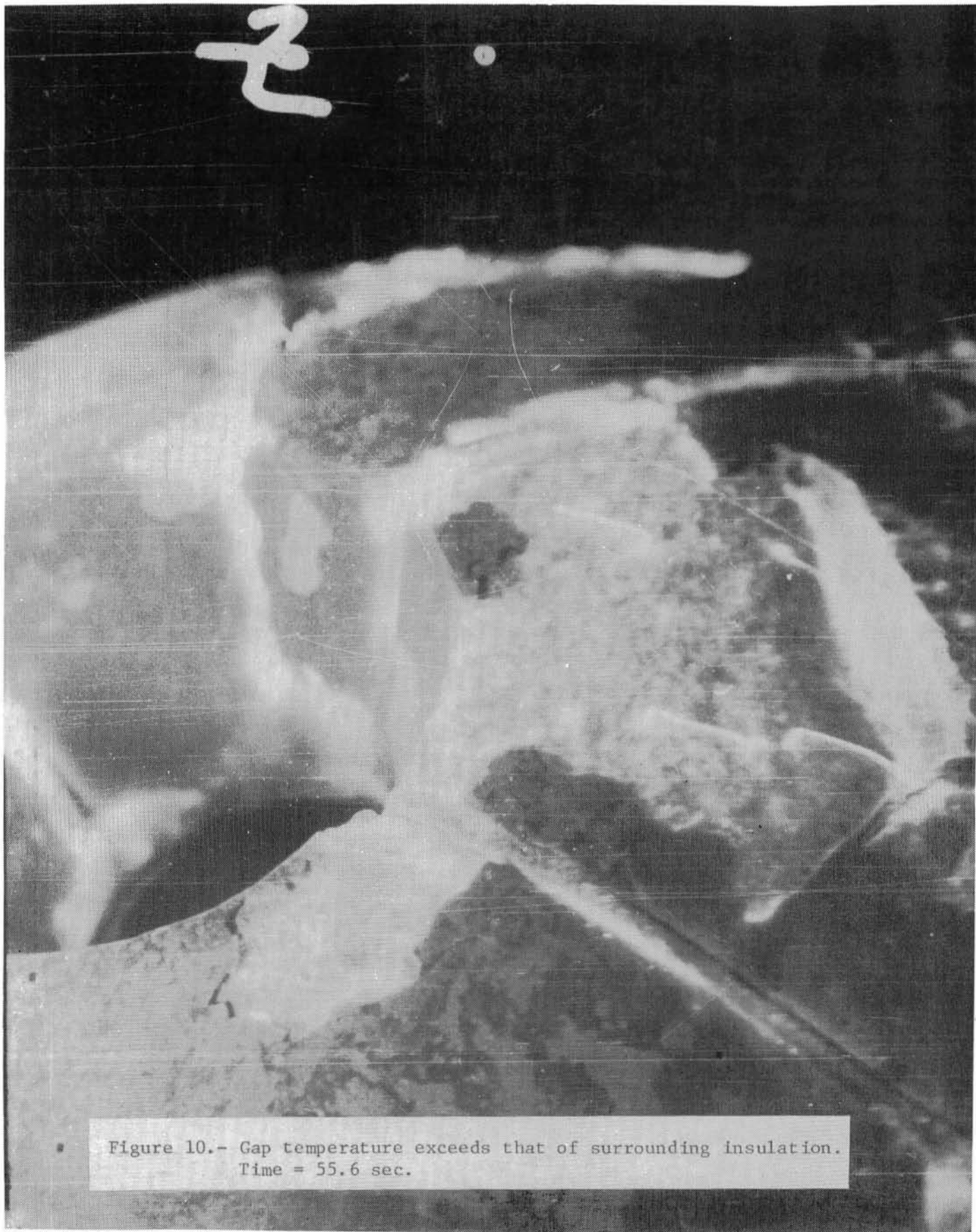Figure 9.- A newly formed gap heats up.   Time = 53.6 sec.

Figure 10.- Gap temperature exceeds that of surrounding insulation.
Time = 55.6 sec.

TILE GONE

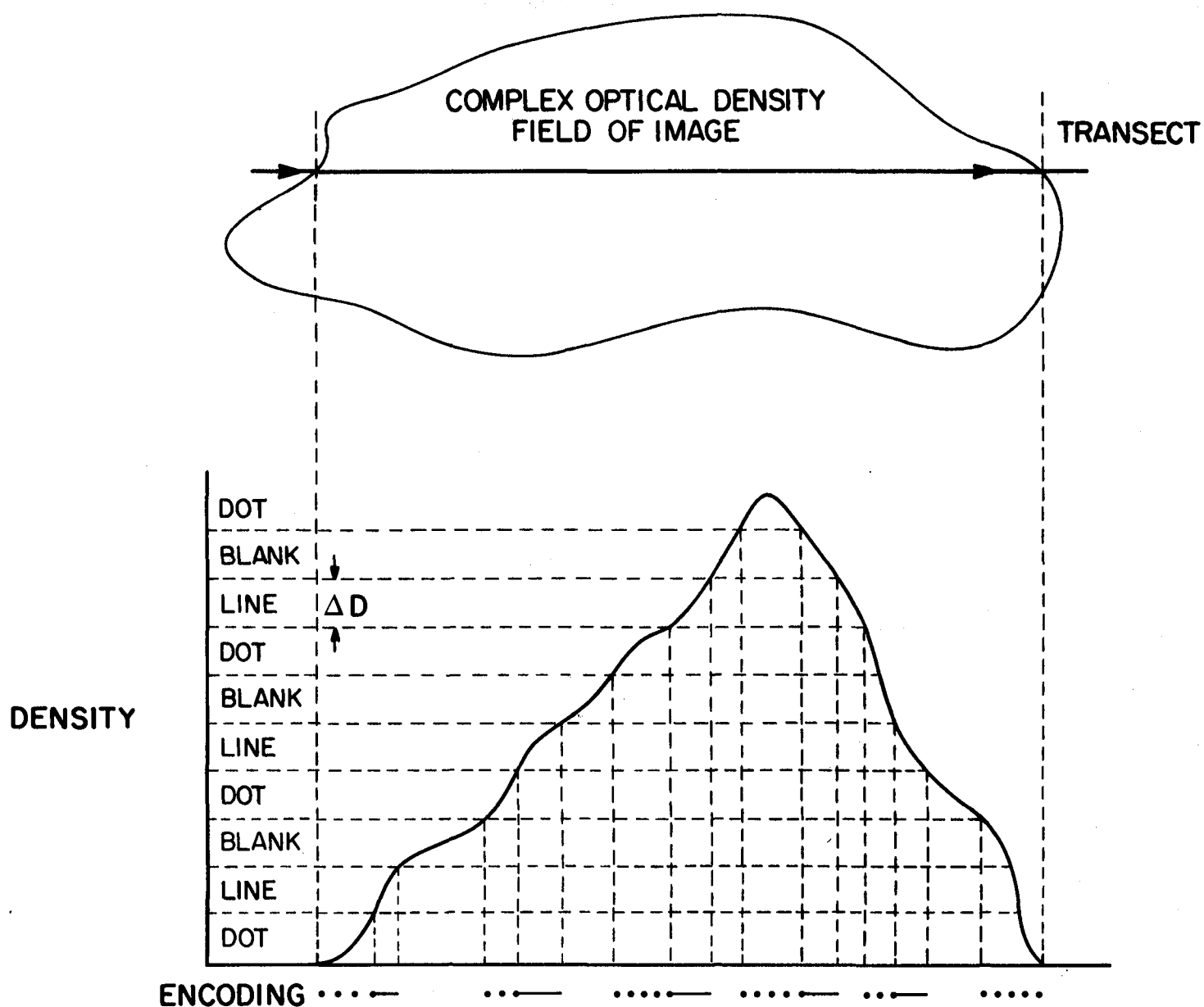Figure 11.- A tile has separated.   Time = 56.6 sec.

COMPLEX OPTICAL DENSITY
FIELD OF IMAGE

TRANSECT

DENSITY

DOT

BLANK

LINE ΔD

DOT

BLANK

LINE

DOT

BLANK

LINE

DOT

ENCODING ···—   ··—   ····—   ····—   ··—   ·····

Figure 12.– Schematic to demonstrate encoding of an optical density field.
The code changes each time the density changes by ΔD. The
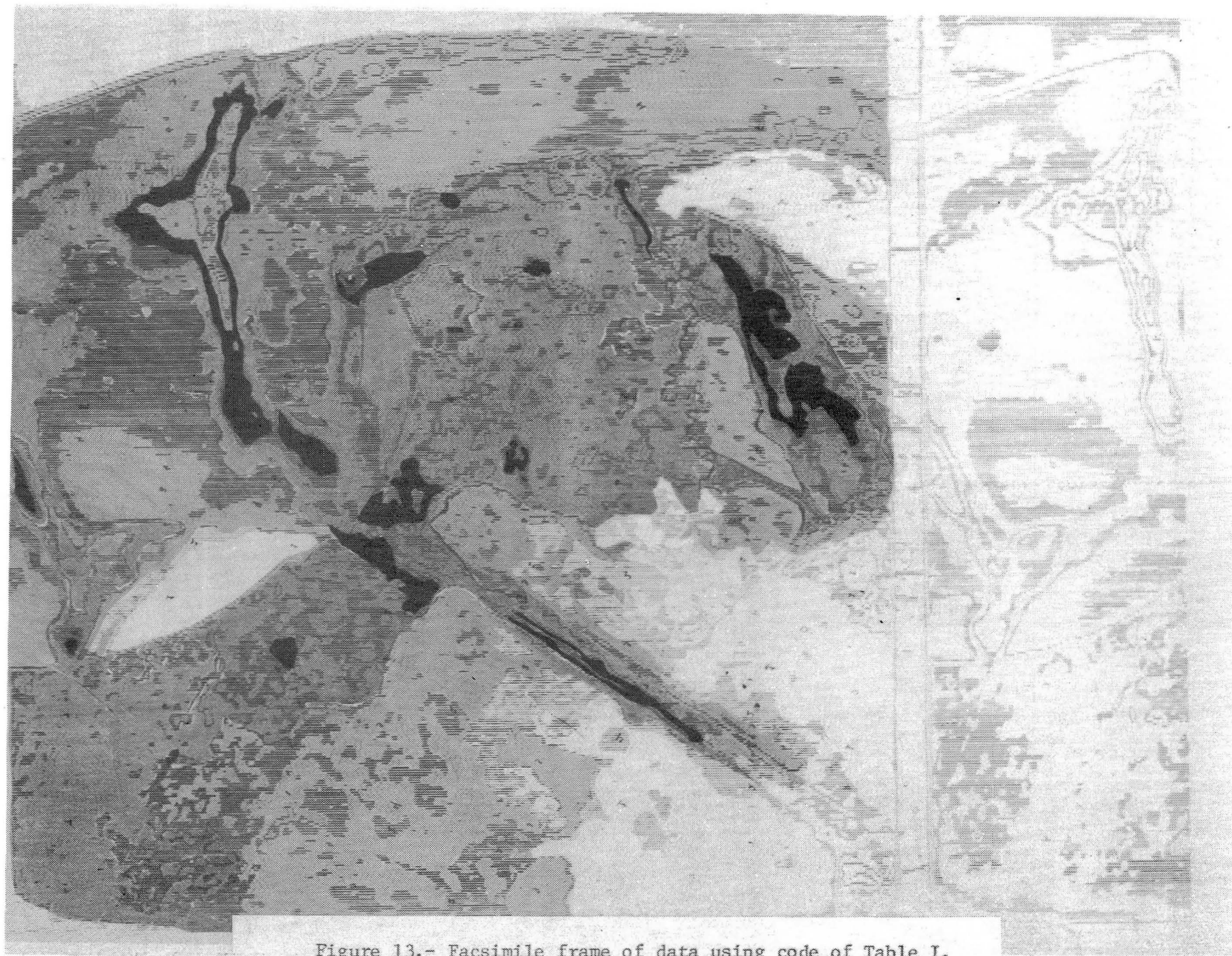sequence blank–dot–line signifies increasing density and
reverses for decreasing values.

Figure 13.- Facsimile frame of data using code of Table I.

1. Report No. TM-83237	2. Government Accession No.	3. Recipient's Catalog No.
4. Title and Subtitle USE OF A VARIABLE EXPOSURE PHOTOGRAPHIC PYROMETER TO MEASURE SURFACE TEMPERATURES ON A HEMISPHERICAL-FACE MODEL		5. Report Date April 1982
		6. Performing Organization Code
7. Author(s) Andronicos G. Kantsios, William C. Henley, Jr., and Walter L. Snow		8. Performing Organization Report No.
9. Performing Organization Name and Address NASA Langley Research Center Hampton, VA 23665		10. Work Unit No. 506-53-33-02
		11. Contract or Grant No.
12. Sponsoring Agency Name and Address National Aeronautics and Space Administration Washington, DC 20546		13. Type of Report and Period Covered Technical Memorandum
		14. Sponsoring Agency Code

15. Supplementary Notes

16. Abstract

Remote surface temperature measurement devices have come into common usage in the past few years. The use of infrared devices in satellite measurements, ground wind tunnel facilities, and industry have clearly proved advantageous. One early instrument in this measurement area (especially in wind tunnel/arc tunnel work) has been the photographic pyrometer. When used for the visible portion of the spectrum the technique is limited to the high temperature range where objects become self luminous. For such cases, the advantage of visible records outweigh many of the disadvantages of working with film. The paper will discuss recent innovations which promise to make the readup more tractable.

17. Key Words (Suggested by Author(s)) instrumentation pyrometer temperature	18. Distribution Statement Unclassified - Unlimited Subject Category 35

19. Security Classif. (of this report) Unclassified	20. Security Classif. (of this page) Unclassified	21. No. of Pages 25	22. Price A02